International Statistical Review

International Statistical Review (2022) doi: 10.1111/insr.12486

Nudging a Pseudo-Science Towards a Science—The Role of Statistics in a Rainfall Enhancement Trial in Oman

Ray Chambers[1], Stephen Beare[2], Scott Peak[3] and Mohammed Al-Kalbani[4]

[1]*National Institute for Applied Statistics Research Australia, University of Wollongong, Wollongong, NSW, Australia*
E-mail: ray@uow.edu.au
[2]*Analytecon, Berry, NSW, Australia*
[3]*Australian Rain Technologies, Sydney, NSW, Australia*
[4]*Trading and Investment Establishment, Muscat, Oman*

Summary

Although cloud seeding is a commonly used and plausible method for rainfall enhancement, its practical efficacy has not been established for seeding of convective clouds with hygroscopic materials. Other methods of rainfall enhancement are viewed as much less plausible. Thus, although increased electrical charge has been shown to enhance precipitation in cloud chamber experiments, exactly how ionisation of clouds can increase rainfall in the open atmosphere remains conjectural. A trial of the efficacy of ionisation for rainfall enhancement in the Hajar Mountains of Oman was carried out over 2013–2018. This paper provides some background to this non-mainstream approach to increasing rainfall, showing how statistical modelling of rainfall data might be used to nudge rainfall enhancement via ionisation towards a more scientifically acceptable status. Analysis of the data collected in the trial shows that ionisation led to a statistically significant enhancement in positive rainfall in gauges located up to 70 km downwind of the ionisers. A headline analysis specified prior to commencement of the trial resulted in an estimate of 16.23% enhancement relative to rainfall that would have fallen without any ionisation, while a more sophisticated after the event analysis increased this estimate to 17.64%.

Key words: rainfall modelling; cloud seeding; cloud ionisation; attribution modelling; weather modification; bootstrap simulation; permutation test.

1 Weather Modification and Rainfall Enhancement

A major consequence of a warming global climate is decreasing rainfall in some parts of the world. This is especially true in tropical and semi-tropical regions, with huge implications for food production for much of the world's population. Consequently, there is an increasing interest in geoengineering solutions to this problem, including weather modification.

Weather modification technology typically aims to increase the amount of rain that falls to the ground when it does rain. This is usually referred to as rainfall enhancement. Note that this should not be confused with 'making it rain'. There is no scientifically supported basis for

conjuring rainfall out of a moisture-free environment. However, there is evidence that human intervention into the formation of water droplets in moisture-laden clouds can lead to an increase in subsequent rainfall. Cloud seeding, which is usually carried out by the injection of chemicals into these clouds, has been the subject of extensive scientific investigations over the last 70 years. See https://www.uaerep.ae/en/app/3 for an ongoing programme of research in this area. But although there have been, and continue to be, many cloud seeding programmes aimed at enhancing rainfall in different parts of the world, the scientific case for their efficacy remains somewhat murky. This is because rainfall on the ground is usually measured using rain gauges, and these are typically not optimally placed for evaluation of an enhancement effect. Furthermore, the large natural spatial and temporal variability in rain gauge measurements makes it extremely difficult to determine whether any enhancement has occurred or whether these measurements correspond to rainfall that would have occurred anyway, regardless of any enhancement effort.

To overcome this variability, much of the published analysis of cloud seeding experiments has focussed on identifying an enhancement effect using suitably averaged rain gauge data, for example, by averaging daily rainfall values over a specified area and or over a specified time interval, and then comparing these average values for times when cloud seeding has been carried out with times when no such seeding has occurred, often by evaluating ratios of these averages. Because averaging reduces variability, this has the benefit of substantially reducing the noise in the gauge level data. However, it has at least two major drawbacks. The first is that the consequent reduction in sample size means that the degrees of freedom available for identifying an enhancement effect are substantially reduced, making it difficult to identify a significant effect. The second is that spatial averaging lumps together gauges that can be exposed to quite different orographic conditions, while temporal averaging lumps together gauge values that are often exposed to quite different meteorological conditions and hence different rainfall regimes. Some examples of orographic variation are variation in elevation and the fact that except in exceptional circumstances, as in large-scale weather events, rainfall is local in nature. In addition, there is the impact of heterogeneity due to different numbers of gauges contributing to the different averages and the spatial non-representativeness of gauges within defined areas due to lack of control over gauge placement in these areas. There is also the necessary restriction to spatio-temporal contextual covariates when attempting to control for variation in factors that are related to rainfall but are unrelated to whether rainfall enhancement procedures were carried out. Consequently, at the time of writing, there is still no strong evidence from average-based analyses that cloud seeding has a significant impact on rainfall on the ground.

In this paper, we take a different approach and use daily gauge-level data to estimate enhancement effects for an alternative approach that uses ground-based ionisation to enhance rainfall. This focusses on actual rainfall in a large network of gauges and has the advantage of maximising the degrees of freedom available for identifying an enhancement effect while eliminating issues arising from spatial and temporal non-representativeness when rainfall data are averaged. It also allows more precise control for spatio-temporal covariates unrelated to enhancement activity that impact on rainfall. The downside, however, is that the method of analysis must be complex enough to be able to deal with extremely variable gauge-level rainfall data, while also providing robust estimates of rainfall enhancement, together with associated measures of statistical confidence, allowing enhancement effects, if present, to be determined with high reliability. Details of our gauge-level analysis methodology are set out in Section 2. In Section 3, we compare cloud seeding and cloud ionisation as rainfall enhancement methods and summarise current attitudes about their statuses as scientific methods. Then in Section 4, we describe how a series of small-scale experiments in Australia, followed by a larger, and better

instrumented, 6-year experiment in Oman have been used to investigate whether ground-based cloud ionisation actually leads to significant rainfall enhancement. Key results from the Oman experiment are set out in Section 5 and provide strong statistical evidence for this to be the case. Finally, in Section 6, we discuss the impact these positive results could have on the current pseudo-scientific status of cloud ionisation. We note that although the statistical evidence presented here may still be insufficient in this regard, it should help nudge weather modification science towards a better investigation of cloud ionisation as a rainfall enhancement strategy.

2 Estimation of Rainfall Enhancement Using Daily Gauge-Level Data

Rain is a rare event in areas where enhancement is necessary, so gauge-level daily rainfall in these areas is a mix of zero values and positive values, with zero values pre-dominant. Here, it is the positive values, corresponding to the rain that actually falls to the ground, that are of interest, because the aim is to see whether the enhancement technology can make this rainfall more intense, that is increase positive rainfall values. Consequently, we restrict to gauge-level values of positive rainfall when we model enhancement. These positive values are usually highly right-skewed, so all models for gauge-level positive rainfall used in this paper are linear in the logarithmic scale. Furthermore, these values exhibit temporal heterogeneity, even after controlling for known meteorological and orographic characteristics. An important question following use of a rainfall enhancement technology in a low rainfall area is how much of the positive rain observed subsequently is due to use of this technology. This quantity is usually referred to as the attributed rainfall, or just the attribution. In this section, we describe a method for estimating the attribution component of positive rainfall values using a log-scale gauge-level model with temporal random effects.

Let y_{it} denote an observed positive rainfall value and put $LogRain_{it} = \log(y_{it})$. We shall assume that this variable can be adequately modelled as

$$LogRain_{it} = \mathbf{x}_{it}^T\alpha + \mathbf{z}_{it}^T\beta + u_t + e_{it}. \tag{1}$$

Here, i and t are indices for the gauge-day values of positive rainfall, with i corresponding to the observed gauge and t corresponding to the day of observation respectively; $\mathbf{x}_{it}$ denotes the vector valued covariate associated with the fixed effects in the model that are unrelated to enhancement activity, that is, the components of this vector are covariates that are believed to influence the level of 'natural rain' or rain that would have fallen anyway in the absence of any enhancement activity; $\mathbf{z}_{it}$ denotes the vector valued covariate associated with the fixed effects in the model that characterise exposure to enhancement activity, with components that are all zero if the gauge-day observation is one that should not have been impacted by this activity; u_t is a random day effect with zero mean and e_{it} is the model error, also random and with zero mean. Note that it is straightforward to extend 1 to allow for more complex patterns of unobserved heterogeneity. For example, one can easily include a random gauge effect on the right-hand side of 1 if there is reason to believe that significant gauge level heterogeneity exists that is not accounted for by variation in the values defining $\mathbf{x}_{it}$.

The aim is to decompose the observed rainfall for gauge-day it as

$$y_{it} = R_{it}(1 + E_{it}), \tag{2}$$

where R_{it} is the natural rainfall that would have been observed at gauge-day it if there had been no enhancement and E_{it} is the random variable corresponding to enhancement impact. Note that E_{it} can be positive or negative. Furthermore, $LogRain_{it} = \log(R_{it}) + \log(1 + E_{it})$ where, from 1,

$\log(R_{it}) = \mathbf{x}_{it}^T\alpha + u_t + e_{it}$, and $\log(1 + E_{it}) = \mathbf{z}_{it}^T\beta$. It immediately follows that $E_{it} = \exp(\mathbf{z}_{it}^T\beta) - 1$, and using 2, $R_{it} = \exp(-\mathbf{z}_{it}^T\beta)y_{it}$.

We use the standard 'hat' notation to denote estimates derived by fitting 1 to the positive rainfall values in the enhancement data set. There are well-known standard methods for this. Then

$$\widehat{E}_{it} = \lambda\exp\left(\mathbf{z}_{it}^T\widehat{\beta}\right) - 1 \tag{3}$$

and

$$\widehat{R}_{it} = y_{it}\left(1 + \widehat{E}_{it}\right)^{-1} = \lambda^{-1}\exp\left(-\mathbf{z}_{it}^T\widehat{\beta}\right)y_{it}. \tag{4}$$

The constant λ in 3 is typically greater than one and corrects for the bias that arises when we use exponentiation to move from logarithmic scale rainfall to raw scale rainfall. This is because an effect that changes the mean on the log scale has an asymmetric effect on the variance at the raw scale, understating positive residuals and overstating negative residuals. We adapt the smearing approach of Duan (1983) to estimate this parameter.

To motivate how λ is calculated, suppose that the aim is to predict the total amount of rainfall over the set of gauge-days of interest based on 1. Note that this model implies

$$y_{it} = w_{it}d_{it}\gamma_{it},$$

where $w_{it} = \exp(\mathbf{x}_{it}^T\alpha + u_t)$, $d_{it} = \exp(\mathbf{z}_{it}^T\beta)$ and γ_{it} is a positive-valued random variable with expectation equal to one whose values are mutually uncorrelated with one another. Because $E(\log(\gamma_{it})) \neq 0$, the naive predictor of raw scale rainfall obtained by back-transformation of the linear predictor based on 1 is

$$\widehat{y}_{it}^{naive} = \exp(\mathbf{x}_{it}^T\widehat{\alpha} + \widehat{u}_t)\exp\left(\mathbf{z}_{it}^T\widehat{\beta}\right) = \widehat{w}_{it}\widehat{d}_{it}.$$

This predictor is biased low. Its bias can be corrected using a smearing adjustment (Duan 1983), given by $\widehat{y}_{it}^{adj} = \mu\widehat{y}_{it}^{naive}$, where $\mu = n^{-1}\sum_{i't'}\left(y_{i't'}/\widehat{y}_{i't'}^{naive}\right)$ and n is the total number of gauge-days in the set indexed by $i't'$. Next, note that this adjusted estimated value of y_{it} can be decomposed into corresponding adjusted natural rainfall and enhancement components by writing $\widehat{y}_{it}^{adj} = \mu\widehat{y}_{it}^{naive} = (\pi\widehat{w}_{it})\left(\lambda\widehat{d}_{it}\right)$ where $\pi > 1$, $\lambda > 1$ and $\pi\lambda = \mu$. Because there is no obvious way of defining these component adjustments, we take a pragmatic approach, setting $\lambda = 1 + a$ and $\pi = 1 + ma$ where m is a suitably chosen positive constant. Because $\mu = 1 + r$, where $r > 0$ is known, it follows that we must have $a + ma + ma^2 = r$, and solving for a, we obtain

$$a = \frac{\sqrt{(1+m)^2 + 4rm} - (1+m)}{2m}.$$

How to choose m? One choice is $m = 1$, in which case $\lambda = \sqrt{1+r} = \sqrt{\mu}$. Other choices are $m = 0$, in which case $\lambda = \mu$, and $m = \infty$, in which case $\lambda = 1$. Given that the relative sizes of λ and π should reflect the relative difference in the variances of $\widehat{d}_{it}$ and $\widehat{w}_{it}$, we use $m = V(\widehat{w}_{it})V^{-1}\left(\widehat{d}_{it}\right)$ where V denotes empirical variance over the set of gauge-days of interest.

With this definition, we see that if $V(\widehat{w}_{it}) >> V\left(\widehat{d}_{it}\right)$ then $\lambda \approx 1$, that is, there is virtually no transformation bias adjustment for the estimated enhancement attributions, while if the reverse holds then virtually all the transformation bias adjustment μ for the fitted values of observed rainfall is concentrated in the estimated enhancement attributions.

Finally, the estimated attribution associated with the gauge-day observation *it* is

$$\widehat{A}_{it} = y_{it} - \widehat{R}_{it} = y_{it}\left(1 - \lambda^{-1}\exp\left(-\mathbf{z}_{it}^{T}\widehat{\beta}\right)\right). \tag{5}$$

These estimated gauge-day attributions can be calculated for any set of gauge-day values of positive rainfall and then summed to give an estimate of the overall attribution due to rainfall enhancement over this set.

3 Chemical Cloud Seeding Versus Ionisation of Moisture-Laden Clouds

The basic idea underpinning cloud seeding is that the injection of chemical particles into a moisture-laden cloud encourages the formation of larger raindrops than would otherwise be the case. In seeded glaciogenic clouds, these chemical particles (usually silver iodide or AgI) serve as ice nucleating particles to form ice crystals and eventually snow, while in warmer convective clouds, they may serve as nuclei for the formation of water droplets, which then collide and coalesce with other water droplets to form raindrops that precipitate out of the cloud. Unfortunately, although recent research (French *et al*., 2018) has shown enhanced snowfall formation in seeded glaciogenic clouds, there remains a lack of strong empirical evidence for increased rainfall on the ground because of seeding of convective clouds. This appears to have motivated at least two influential reviews of rainfall enhancement methods, one by the National Research Council (NRC, 2003) and the other by the World Meteorological Organisation (WMO, 2007; WMO, 2010), to downplay claims that rainfall enhancement via cloud seeding has a strong scientific basis. In particular, the 2010 Statement on Weather Modification by World Meteorological Organisation (WMO, 2010) points out that

- augmentation of precipitation … and other types of cloud and storm modifications by cloud seeding are developing technologies which are still striving to achieve a sound scientific foundation; and
- economic analyses show that rainfall enhancement … could have significant economic benefit, but uncertainties make investments in such efforts subject to considerable risks.

Scientists involved in cloud seeding research have pushed back against this stand (List, 2005), pointing out that it is inappropriate to lump together cloud seeding, which has been shown to consistently work in laboratory-based environments, with other, less well-regarded, and often non-scientific, methods for weather modification. In the case of cloud seeding, the issue is essentially one of demonstrating real-world efficacy and practicality, rather than laboratory-based success, particularly because cloud seeding has a number of drawbacks, including cost (seeding is usually carried out by aircraft or projectile, although ground-based seeding using chemical generators at higher altitudes is also carried out, Manton *et al*., 2017 and Rasmussen *et al*., 2018), lack of suitable seeding opportunities (seeding can be carried out only with certain types of clouds), and potential environmental damage (Hannaford, 2015; Fajardo *et al*., 2016). However, a recent WMO report has pointed out that there is limited scientific evidence for environmental damage, see section 6.7 and 6.9 of Flossmann *et al*. (2018).

The WMO (2010) statement goes further to point out that there is 'considerable evidence that cloud microstructure can be modified by seeding … under appropriate conditions … (but)

evidence for significant and beneficial changes in precipitation on the ground as a result of seeding is controversial, and in many cases cannot be established with confidence'. The statement notes that 'there is statistical evidence, supported by some observations, of precipitation enhancement from glaciogenic seeding' (which induces ice-phase precipitation in very cold clouds), but 'seeding of convective clouds with hygroscopic materials … is not yet an established technology'. This is unfortunate because increasing the number of raindrops by enhancing the coalescence of water droplets in warm convective clouds is viewed as the most effective way of enhancing rainfall in the tropics and semi-tropics.

Cloud seeding is not the only way that water droplets in a cloud can be made to coalesce. Another approach is to 'electrify' clouds by injection of negatively charged particles. The idea is that these electrical charges are transferred to the water droplets in the cloud, with the resulting negatively charged droplets being attracted to neutral droplets in the cloud, thus increasing the number of collisions where subsequent coalescence leads to the formation of raindrops. Although there is both theoretical (Doshi & Agashe, 2015) and laboratory evidence (Yang *et al*., 2018; Zhang *et al*., 2020; Wang *et al*., 2020a, 2020b) that such an 'ionisation' approach to raindrop formation does work, the generally accepted view of most scientists working in weather modification is that it is not a realistic approach—the electrical forces that it depends on are too weak to have any significant influence on the rate of coalescence of water droplets in an actual cloud (Fletcher, 2013). See also section 5 of Levin (2009) and section 3.5.1 of Flossmann *et al*. (2018).

But this has not stopped scientists with an interest in weather modification trying out various techniques for ionisation of clouds. The first of these attempts (led by Bernard Vonnegut and Charles Moore and colourfully described in Dempewolff 1959) was carried out in the late 1950s. Although the results of these experiments were promising (Vonnegut & Moore, 1959; Vonnegut *et al*., 1961, 1962a, 1962b), they were inconclusive, and rainfall enhancement via AgI-based cloud seeding became the dominant paradigm.

The lack of uptake of the ionisation idea by the weather modification community in the West did not stop scientists in other parts of the world continuing their investigation into cloud ionisation as a method of rainfall enhancement. In particular, there was work carried out on ionisation technology within the Soviet Union. Unfortunately, details of what was achieved

Figure 1. *An early photograph of a ground-based ioniser installation. Its location is uncertain, but on the basis of the accompanying documentation, it is likely that the photograph was taken in Russia before 1999.*

were not published in accessible journals. It was only in the early part of the current century that people who had been part of this work started promoting it. One of these was Valery Uibo, who is credited with the development of a ground-based rainfall enhancement technology that uses atmospheric uplift to artificially ionise clouds (Figure 1). However, promotion of this technology was not via the usual scientific channels. Instead, it was carried out entrepreneurially, via commercial channels, and aimed at organisations and institutions facing weather-related risk. Given that there was no prior record of any scientific assessment of ground-based ionisation, it is understandable that there was a considerable amount of scepticism about its efficacy, particularly by scientists working on cloud seeding. This was not helped by rather overblown claims by its promotors about the ability of the technology to 'create' rain from desert air (Hsu & Bryner 2011).

Because ionisation had been a promising avenue for rainfall enhancement before the development of ground-based ioniser technology, there does not seem to be any good reason to dismiss the potential efficacy of ground-based ionisation because of its rather unconventional promotion. In particular, the basis of the approach is cloud ionisation via atmospheric uplift, which is hypothesised to work as follows:

1. aerosols (small atmospheric dust particles) become negatively charged (ionised) after exposure to a high-voltage corona discharge wire array (the ioniser);
2. convection currents and turbulence in the atmosphere then convey these negatively charged aerosols into the cloud layer where they act as cloud condensation nuclei (CCN) for cloud droplets;
3. the electric charge carried by these CCN-generated cloud droplets stimulates their collision with other cloud droplets and subsequent coalescence into raindrops; and
4. this increased rate of coalescence has a significant positive effect on the amount of rainfall from clouds downwind of the ioniser.

It is step 3 that is controversial, because some atmospheric physics models for the effect of electric charge on the interaction of cloud droplets (Fletcher, 2013, 2014) indicate that this coalescence cannot happen to any sufficient extent to impact on raindrop formation. But these results are disputed (Tinsley & Zhou 2014), and there are recent studies that are more supportive of the link between ionisation and droplet coalescence (Wang *et al*., 2020b). In this context, it seems reasonable to ask for strong empirical evidence supporting the efficacy of ground-based ionisation, preferably based on properly randomised trials. These results have recently become available and are described next.

4 Ground-Based Ionisation Trials

4.1 Australia 2007–2010

The commercial interests that promoted ground-based ionisation as a rainfall enhancement strategy arrived in Australia in 2007. At that time, most of south-eastern Australia was in the grip of a decade long drought, and so there was considerable interest in using this technology where rainfall was particularly needed. This interest translated into five trials of the technology, with the first two in south-east and south-central Queensland, and the remaining three in South Australia, near Adelaide. The Queensland trials over May–June 2007 and January–May 2008 were proof of concept. The South Australian (SA) trials were more focussed on measuring enhancement and were carried out August–November 2008, August–December 2009 and

July–December 2010, with the last two of these carried out as fully randomised trials under the guidance of an independent Scientific Review Panel.

A key aspect of the analysis of the operation of an ionisation technology dependent on atmospheric uplift is identifying the 'footprint' of the system. This is the area where the rainfall enhancement signal, if one exists, should be measurable. It is also an area that changes dynamically as the ionised aerosols created by the system drift downwind. Analysis of data collected in the second Queensland trial indicated that a suitable model for such a dynamic footprint given the wind speeds experienced at the site was a 60° arc oriented in the direction of the prevailing daily steering wind and extending 70 km from the ioniser site. This model was used to define the rainfall enhancement target areas in all three subsequent SA trials.

The first SA trial was essentially an observational study, with the ioniser operated whenever daily weather indices provided by the Australian Bureau of Meteorology showed the potential for significant cloud cover in the target area. The operating schedules used in the second and third trials were specified prior to the start of each trial, however, with the single ioniser used in the second trial randomly turned on and off daily and the two ionisers used in the third trial operated according to a daily schedule defined by a randomised cross-over design. See Chambers *et al*. (2012) for details.

All three SA trials consistently indicated rainfall enhancement of approximately 10% relative to the rainfall that would have fallen in the dynamic target area if the ionisers had not been operated. These results were encouraging, and the Scientific Review Panel recommended that the Australian government carry out further trials to validate them in other locations. However, the long drought in south-eastern Australia came to an end in 2011, and there was no official interest in supporting any further trials.

4.2 Oman 2013–2018

In 2012, the Government of Oman agreed to fund a proof-of-concept trial using two ionisers in the Hajar Mountains of northern Oman in the summer months of 2013. This was followed by funding for a further five-year trial covering the summer months 2014–2018 and focussing on the Hajar Mountains, with the number of installed ionisers increasing by two each year up to a total of 10 by 2017. In the rest of this subsection, we provide an overview of the design and implementation of this study, as well as the data that were collected.

4.2.1 The meteorology of northern Oman and the Hajar Mountains

The Sultanate of Oman is one of the most water-stressed countries in the world, with Intergovernmental Panel on Climate Change (IPCC) simulations showing that the northern part of Oman is expected to face decreasing average annual rainfall in the coming decades of up to 40% (Charabi, 2013). Oman's climate can be divided into two main seasons, separated by transition months. These are the winter or northeast monsoon (December–March) and the summer or southwest monsoon (June–September). Past climatological studies have identified the winter season (December through March) as accounting for the bulk of rain in flat and coastal areas in northern Oman. Troughs, depressions and the occasional tail end of cold fronts move through the region from the west and northwest resulting in large-scale systems that can provide significant rainfall. However, the occurrence and amount of rainfall is highly variable with no rain at all in some years.

During the summer season, convective rainfall over the Hajar Mountains is a locally observed phenomenon with reported high occurrence of storms. This rainfall is generally due to a diurnal sequence of events (US Marine Corps, 1990). Low to mid-level south-westerly winds bring monsoonal moisture up through the Gulf of Oman, and the differential rates at which the land

mass and the sea heat up over the course of the morning then create low pressure over the land surface and give rise to a sea breeze circulation. The Hajar mountains in northern Oman run parallel to the coast of the Gulf of Oman and have peaks of over 3 000 m. This sea breeze circulation is enhanced by convection up the steep slopes of these ranges and the strengthening of the low pressure on the windward side of these mountains as they warm relative to the air mass at the same elevation. This results in cloud formation and rainfall over the ranges, which then dissipates over the lee side of the ranges and the desert. This convective weather behaviour makes summer a suitable time for uplift dependent rainfall enhancement in the Hajar Mountains.

4.2.2 Ioniser deployment

The trial commenced with the deployment of two ionisers, labelled H1 and H2, respectively, in the Batinah/Dakhliyah Region of Oman in 2013. This region was chosen considering synoptic and local wind flows, cloud types, widespread uplift and moisture availability. Such features affect the delivery of ionised aerosols to the cloud layer and potential subsequent rainfall enhancement. The sites for H1 and H2 were chosen so that they were both at high elevation (2 670 and 2 157 m, respectively) and as similar as possible in terms of meteorological conditions, but sufficiently separated to ensure no overlap of a rainfall enhancement effect. An extra two ionisers were then deployed each subsequent year of the trial up to and including 2017. These were at lower elevations (984 to 1 876 m) and were sequentially labelled H3 and H4 in 2014, H5 and H6 in 2015; H7 and H8 in 2016; and H9 and H10 in 2017. The additional ioniser sites were generally positioned either side of ionisers that were already in place, with sites chosen to be sufficiently separated from one another, ensuring their footprints did not significantly overlap and effectively covering the main north-west to south-east range of peaks in the Hajar

Figure 2. *The different ioniser designs used in the Hajar Mountains trial. Top row is the original pyramid design at H2 (left) and fisheye design used at H3 (right). Bottom row is the fisheye design used at H7 (left) and triangle design used at H10. These design modifications aimed to increase the amount of ion flux generated when the device is operating.*

Mountains. Summer winds in northern Oman are often from the NE, so the ionisers were effectively deployed along a line running at 90° to the usual direction for winds in the Hajar Mountains and located to take advantage of orographic lifting of the ionised aerosols generated by their operation. Figure 2 shows the three different ioniser designs that were used in the Hajar Mountains trial, while Figure 3 shows the locations of H1–H10.

4.2.3 Ioniser operation

Ionisers were remotely switched on or off daily from the trial operations centre in Muscat, irrespective of daily meteorological conditions, and according to a randomised operating schedule that was specified at least 2 months prior to the commencement of the trial each year. The design of the schedule depended on the number of operating ionisers that year and is summarised in point format below. In all cases, there was a nominal switching time of 7 am to ensure enough time to allow ionised aerosols to be transported downwind before the onset of convective cloud development around 10 am. A 30-min temporal buffer was also added to the switch time, so that the ionised aerosols from ionisers being switched off for the day had time to clear before operating ionisers for the day were switched on.

- **2013**: Two ionisers (H1, H2) were operated in 2013 and the trial covered the 170 days from 15 May to 31 October. They were operated using an alternating schedule that constrained H1 to be on for 85 randomly chosen days while H2 was off and vice versa.
- **2014**: Four ionisers (H1–H4) were operated in 2014 and the trial covered the 140 days from 1 June to 18 October. This period was partitioned into 10 temporal blocks, each of 14 days, and spatial pairing was used to ensure neighbouring ionisers did not operate simultaneously, with H1 paired with H4 and H2 paired with H3. Pairs were randomly turned on and off so that over

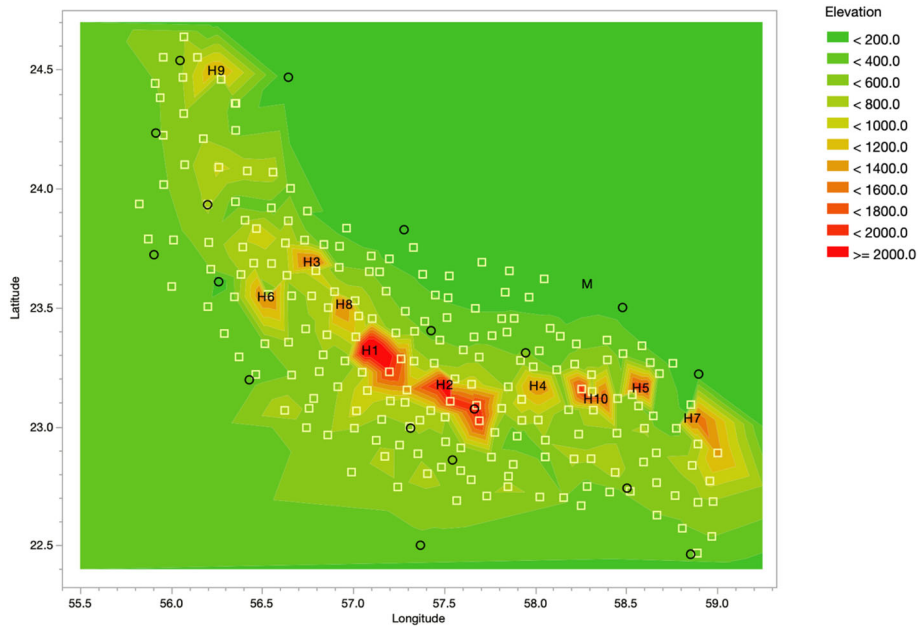

Figure 3. *Contour map of elevations (m) in the Hajar Mountains trial area. Locations of ionisers (H1–H10), rain gauges (light coloured squares) and automatic weather stations (open circles) are superimposed. The point marked 'M' is Muscat International Airport.*

any 14-day period each pair was operated seven times, and over the 140-day trial each pair was operated 70 times.

- **2015**: Six ionisers (H1–H6) were operated in 2015, with the trial designed to commence 1 June and to complete 18 October (140 days), with three mechanisms operated each day. There are 20 combinations of operating states that satisfy this constraint, so the design period of 140 days was partitioned into seven blocks of 20 days, with these 20 combinations then randomly allocated to days within each block, ensuring that each ioniser was operated for 70 days over the 140 days of the trial. Although mechanical issues delayed the start of the trial to 14 June (restricting the actual trial period to 127 days), the operating sequence commenced 1 June as designed.
- **2016**: The trial involved eight ionisers (H1–H8) and was planned for 1 June to 31 October (H1–H6) and 1 July to 31 October (H7, H8). A spatially and temporally balanced approach to specification of their operating schedule was adopted, satisfying the three constraints: (i) the same number of deployed ionisers to be operated/not operated each day; (ii) no ioniser to be operated for more than 2 days in a row; and (iii) no more than two contiguous ionisers to be operated on any day, with contiguity defined in terms of a NW to SE ordering, There are 28 possible configurations of daily operating statuses for six ionisers, and 68 possible configurations of daily operating statuses for eight ionisers that satisfy these constraints. These were randomly sampled with replacement to obtain a design that covered the 30 days 1 June to 30 June for H1–H6 and the remaining 123 days 1 July to 31 October for H1–H8. This process was then independently repeated a very large number of times, with the final design chosen so that it provided the minimum number of times an ioniser was operated 2 days in a row over the 153 trial days. This operating sequence was followed from 1 June even though there were delays in bringing H7 and H8 online in July.
- **2017**: The trial involved 10 ionisers (H1–H10) and was designed to cover the period 1 July to 31 October (123 days). As with the 2016 design, a spatially and temporally balanced design satisfying conditions (i)–(iii) was chosen, based on the 168 possible configurations of daily operating statuses for 10 mechanisms satisfying these constraints. Repeated random sampling of these eligible configurations to minimise the number of times an ioniser was operated 2 days in a row was used to identify the final design.
- **2018**: This final year of the trial in the Hajar mountains did not involve any new installations and covered 1 July to 31 October (123 days). The design of the trial was therefore identical to that used in 2017, with the operating schedule specified by an independent repetition of the same random sampling process as used in 2017.

4.2.4 Rainfall measurement

Due to the localised and short-lived nature of rainfall throughout the Hajar Mountains trial area, and because there were a limited number of automatic weather stations maintained by the Oman Directorate-General of Meteorology and Aerial Navigation (DGMAN) in the area, an array of 120 automatic rain gauges was installed prior to the start of the 2013 trial. These gauges were installed on an approximate 10 km regular grid throughout the trial area and provided daily rainfall data that was remotely recorded by the trial operations centre in Muscat. Deployment of additional ionisers over 2014–2017 required installation of additional rain gauges (as well as redeployment of 12 installed gauges in 2014) to cover the corresponding extension of the trial area. By 2017, the rain gauge network covering the Hajar Mountains trial area was made up of 201 gauges (Figure 3). No new gauges were installed in 2018 because no new mechanisms were deployed in the Hajar Mountains that year.

4.2.5 Meteorological data on weather conditions

To a large extent, prevalent meteorological conditions dictate rainfall at any gauge and on any day. These conditions exist independently of whether an ioniser is operated in the vicinity of that gauge on that day. Consequently, it is important that analysis of the impact of the operation of these mechanisms also controls for the influence of day-to-day change in meteorological conditions on observed rainfall. Furthermore, the hypothesised rainfall enhancement process underpinning their use depends on direction and speed of the local steering winds, in the sense that the footprint, that is, the area over which rainfall enhancement is expected, is hypothesised to be downwind of the installed location and to extend as far as wind speeds can transport the ionised aerosols. Having access to sufficient meteorological information to determine the direction and speed of the daily steering wind is therefore crucial in any rigorous assessment of efficacy of this type of ground-based ionisation.

There were two sources of meteorological covariates associated with rainfall propensity in the trial area each day, that is, rainfall unrelated to operation of the ionisers. The first was the data collected by the automatic weather stations (AWS) operated by DGMAN in the Hajar mountains area. Their locations are shown in Figure 3. Hourly observations from these stations were used to characterise prevailing weather conditions on the day. Note that not all AWS in the trial area were used in each year, due to data availability problems. The main measurements collected from each AWS and used in the analysis of the trial data were:

- wind speed (m/s);
- dry air temperature (°C);
- dew point temperature (°C);
- relative humidity (%); and
- air pressure (hPa) at AWS ground level (i.e. QFE air pressure).

Daily averages of these measurements were used in the analysis of daily rainfall in the trial area. Because cloud formation in the Hajar mountains is essentially a late morning and afternoon phenomenon, these averages were computed using readings from 10:00 to 20:00 inclusive.

The second source of meteorological covariate information was the daily DGMAN radiosonde at the international airport at Muscat, Oman. This radiosonde is used to collect daily data on vertical wind profiles (direction and speed) as well as the values of key meteorological indices thought to be predictive of rainfall propensity in northern Oman. Following standard meteorological requirements, the radiosonde is usually launched around 4 am daily, with data from it used to define steering wind speed and direction each day. Given the elevation of some of the ioniser locations in the Hajar Mountains, and particularly H1 and H2, a decision was made prior to analysis of data collected in the 2013 trial to define the daily steering wind direction and speed as the average wind direction and speed going from the 700 hPa to the 500 hPa pressure levels in the vertical wind profile data collected by this radiosonde. In 2015, 2017 and 2018, an extra daily radiosonde was launched aimed at investigating whether wind directions later in the day were informative in terms of identifying the actual direction of air transport over the Hajar Mountains. This led to the conclusion that wind directions later in the morning were essentially the same as those measured using the 4 am radiosonde, while winds in the afternoon were often in an offshore direction and irrelevant to air transport over the trial area.

In addition to information on vertical wind profiles, radiosonde data are used to compute key daily meteorological indices that are indicative of general rainfall propensity on the day. The most important of these were identified as

- total totals index (total.totals): an indicator for storm development;
- lifted index (lifted.index): an indicator for thunderstorm development;
- precipitable water (prec.water): the amount of rainfall if a column of the atmosphere were to be precipitated; and
- lifted condensation level (lcl.pres): a measure of cloud base height.

Over 2013–2014, the radiosonde data were generally of good quality, with occasional missing days due to operational issues. In such cases, model-based imputation was used to 'fill in' these data. However, between 2016 and 2018, there were extended periods of missing radiosonde data due to changes in the radiosonde technology used by DGMAN. These missing data were assumed to be missing completely at random and so these periods were excluded from the trial.

There were two main imputation methods used for the missing radiosonde data. When wind speed and direction data were missing from one radiosonde on a day, but these data were available from another later (or earlier) radiosonde, then a bivariate Gaussian distribution was fitted to the radial components of wind direction and speed for days where both radiosondes provided data. This distribution was used to impute the missing radial values as the expected values of the missing components given the observed components for the same day.

When there was no radiosonde data for the day, and there were no more than three consecutive days of missing radiosonde data, the missing data were imputed using observed data from the same radiosonde, assuming that they were missing at random given these observed data. This was carried out via a type of twiced non-parametric trend estimation for both radial components. A locally linear trend using a default bandwidth was first computed for each component. Residuals from this trend were then re-smoothed using a smaller bandwidth than the original to define a trend correction. Finally, both the original trend and the trend correction were added together to produce predicted values for the missing components.

Both methods of imputation for missing radial values were followed by back transformation to obtain corresponding imputed wind direction and speed values, with missing data on meteorological indices imputed similarly. As already noted earlier, longer periods of missing radiosonde data were excluded from the trial. This resulted in actual or imputed radiosonde data from the 4 am Muscat radiosonde being available for a total of 740 trial days 2013–2018. Table 1 shows the number of such days for each year of the trial. The large amount of missing data over 2016–2018 is evident.

In Figure 4, we show the distribution of steering wind directions over 2013–2018 when these are categorised according to one of eight principal directions. Here, NNE corresponds to a wind direction between 0° and 45°, ENE is 45° to 90°, and so on, until NNW which is 315° to 360°. The main wind directions experienced in the trial were NNE and ENE, that is, the prevailing steering winds were from the NE. Interestingly, the distribution of median positive gauge level rainfall by wind direction that is also shown in Figure 4 indicates that the heaviest rainfall tended to occur when the steering winds were more southerly and westerly, suggesting occasional strong monsoonal events.

Table 1. *Impact of missing radiosonde data 2013–2018.*

Year	*2013*	*2014*	*2015*	*2016*	*2017*	*2018*
Trial period (days)	15/5–31/10 (170)	1/6–18/10 (140)	14/6–18/10 (127)	1/6–31/10 (153)	1/6–31/10 (153)	1/7–31/10 (123)
Missing days imputed	24	23	26	26	24	16
Days used in analysis	170	140	127	125	108	70
Missing days excluded	0	0	0	28	45	53

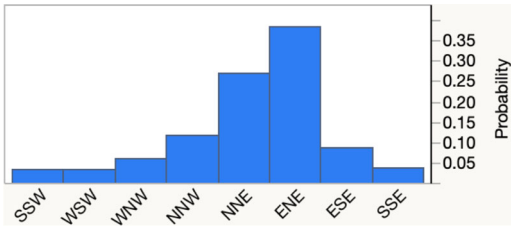

Direction	Distribution 2013-2018 (per cent)	Median Positive Gauge Rainfall (mm)
SSW	3.1	1.8
WSW	3.2	2.4
WNW	5.8	2.2
NNW	11.4	1.6
NNE	26.8	1.6
ENE	38.1	1.4
ESE	8.2	0.8
SSE	3.4	3.8

Figure 4. *Distribution of 2013–2018 directions of daily steering winds (4 am radiosonde at Muscat) over the 740 days when these data were available (or could be imputed). Median values of positive gauge level rainfall for these days classified by wind direction are also shown.*

Table 2. *Correlations of daily values 2013–2018 of meteorological indices with proportion of gauges reporting rainfall (rainfall event) and average gauge-day positive rainfall (positive rainfall) on days when there was rainfall.*

	lifted.index	*total.totals*	*lcl.pres*	*prec.water*
Rainfall event	−0.394	0.416	0.202	0.388
Positive rainfall	−0.414	0.395	0.335	0.485

Table 2 shows the correlations between the four main meteorological indices indicative of rainfall propensity and average gauge-day positive rainfall for the 549 (out of 740) days when there was rainfall reported in the trial area. We see that all four indices correlate with both the occurrence and the amount of actual rainfall. However, the correlation is not strong, averaging between 30% to 40% in absolute value and with the highest value (0.485), unsurprisingly, being the correlation between Precipitable Water and Positive Rainfall. Although not strongly predictive of rainfall, this implies that these indices may be useful as indicators of rainfall potential and so should be considered as control variables in any analysis of actual rainfall.

4.2.6 Daily rainfall

The rain gauge network installed across the Hajar Mountains 2013–2017 (Figure 3) provided hourly rainfall readings at each gauge, for each day of the trial. These hourly readings were summed to provide 122 259 daily gauge-level rainfall values for each of the 740 trial days when steering wind direction data are available. In what follows, we define a gauge-day rainfall value as the total amount of rainfall recorded at a gauge on a day. Given the arid conditions that are prevalent across the Hajar Mountains trial area, it is not surprising that most (approximately 92.5%) of the rainfall readings for these gauge-days are zero, with a corresponding overall average gauge-day rainfall of 0.35 mm. However, from a rainfall enhancement viewpoint, it is the amount of rain that falls to the ground that is of interest, because the main hypothesis underpinning the trial of the ioniser technology in the Hajar Mountains is that it can make rainfall more intense, that is, increase this amount. Over the 740 days of the trial the average gauge-day value of positive rainfall, that is, where rainfall in a gauge was greater than zero, was 4.74 mm.

This average value conceals a lot of gauge-to-gauge and day-to-day variability. In Figure 5, we show the histograms of gauge-day values of *LogRain* over 2013–2018 for all gauge-days with positive rainfall and for downwind gauge-days only. These exhibit the characteristic feature of gauge-level rainfall, with many measurements at the lowest levels of gauge measurement capability (0.2 and 0.4 mm, or log scale values of −1.61 and −0.92) and with comparatively few measurements above 20 mm (log scale = 3.00). The spatial and temporal complexity of the Hajar Mountains gauge-day rainfall over 2013–2018 is then illustrated in Figure 6 by bubble plots of the gauge-day values of positive rainfall for each year of the trial and for the different gauge locations defining the gauge network that year. These bubble plots graphically illustrate the drying out of the trial area from 2016 (echoed by the decreasing values of average gauge-day positive rainfall), as well as the expansion of the gauge network each year.

5 Statistical Analysis of the 2013–2018 Trial Data

5.1 The Headline Statistical Analysis

The headline statistical analysis of the Oman trial data was specified before inspection of the first tranche of rainfall data collected in 2013. This analysis defines the 'official' statistical estimates produced by the data collected in the trial, including the estimated rainfall enhancement over the trial period. It is based on the analysis used in the 2009 and 2010 trials in South Australia (Chambers *et al.*, 2012), with the main difference being the definition of the shape of the rainfall enhancement footprint. Recollect that this is the region downwind of the site of an operating ioniser where a rainfall enhancement effect (if such an effect exists) would be expected to occur. Note that this footprint is dynamic, in the sense that its orientation (but not its shape) can vary from day to day depending on the direction of the prevailing winds.

In South Australia (SA), the footprint was modelled as the sector of a circle, with origin at the ioniser site, a 60° internal angle and with a central axis oriented downwind in the direction of the daily steering wind. The radius of the sector was held fixed at 70 km because this was judged a sufficient maximum distance for ionised aerosols to be carried downwind given steering wind speeds on a day. The daily steering wind direction and speed was defined by

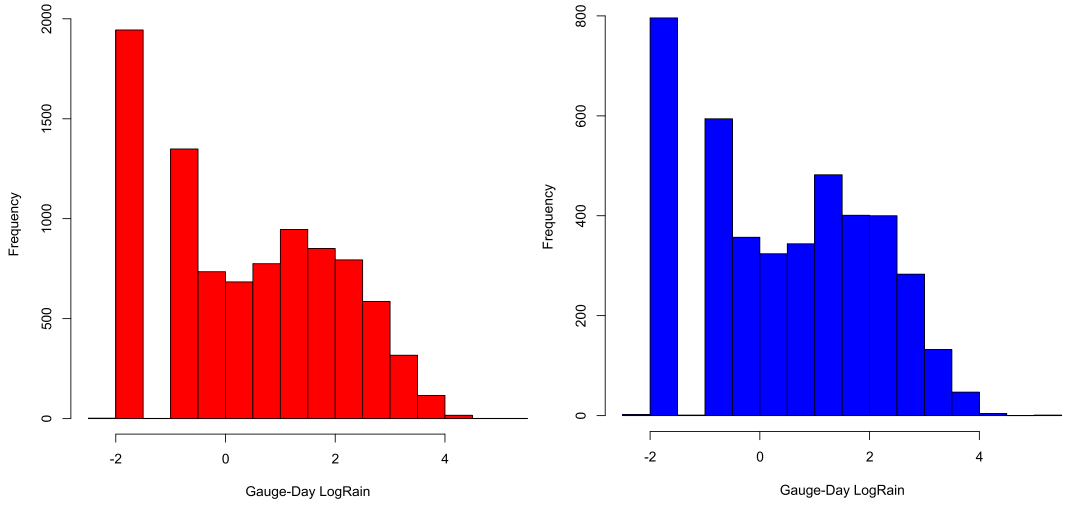

Figure 5. *Histograms of distributions of gauge-day values of LogRain, 2013–2018. The plot on the left is for all such values, while the plot on the right is restricted to downwind gauge-day values.*

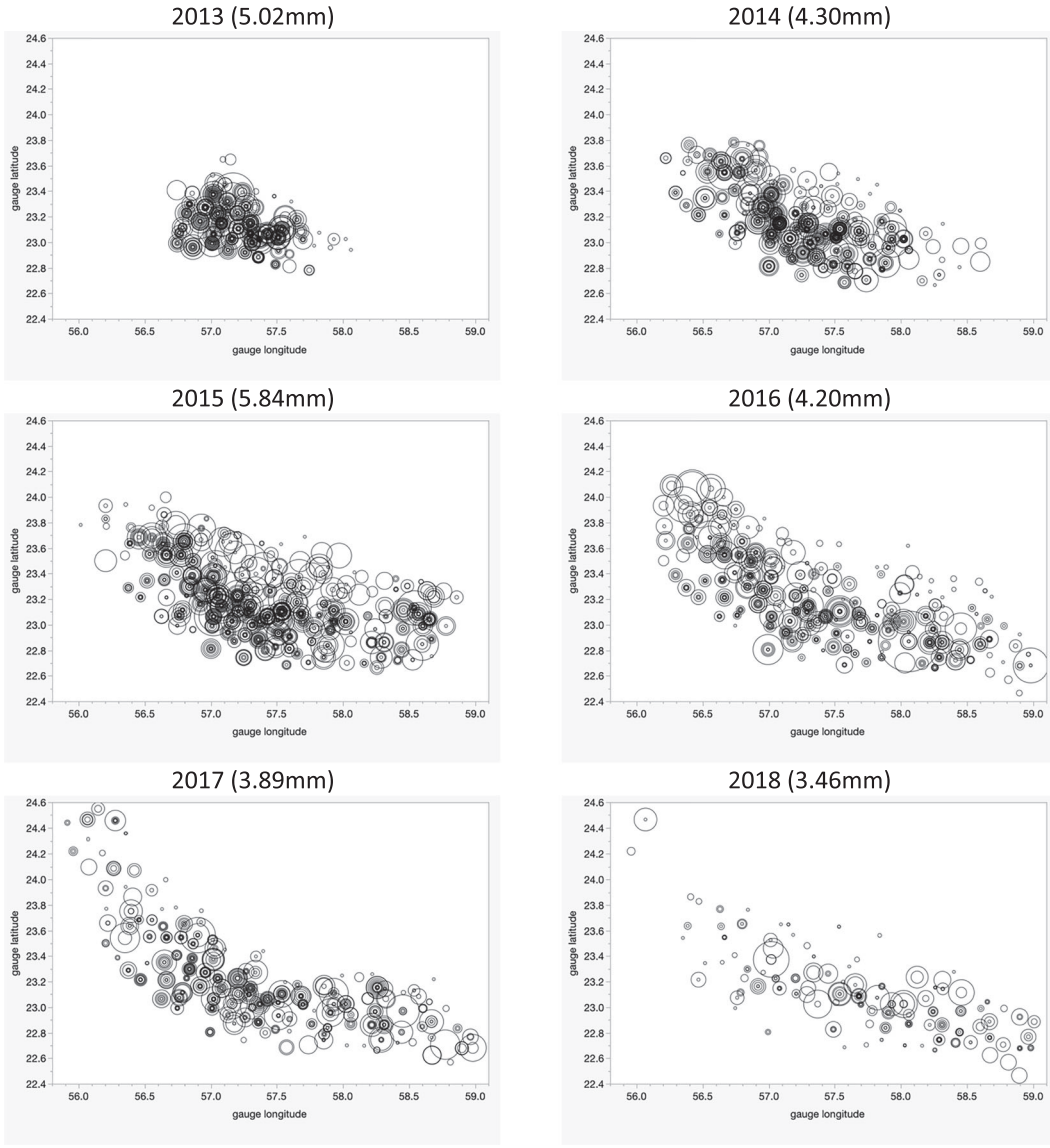

Figure 6. *Bubble plots of gauge locations showing 2013–2018 spatial distributions of gauge-day values of positive rainfall. The addition of more gauges each year up to 2017 can be seen in the increasing spatial extent of the data. Annual average values of gauge-day positive rainfall shown in parentheses. The larger the circle in each plot, the larger the corresponding rainfall measurement at the gauge relative to other rainfall measurements in that year.*

speed weighted averaging of the 850 to 700 hPa wind directions and speeds as measured by the daily radiosonde launched from Adelaide airport.

Inspection of 2013 radiosonde data from Muscat airport indicated that the SA footprint model needed to be modified to take account of the higher elevations of the first two ionisers (H1 and H2) deployed in the Hajar Mountains and the quite different wind speeds and topography compared with SA. The footprint used in Oman was specified to be a 30 km wide rectangular corridor with central axis originating from the ioniser site and extending 70 km downwind from the site in the direction of the daily steering wind. The definition of the daily steering wind

was also changed to correspond to higher altitude winds, defined as the speed weighted average of the 700 to 500 hPa winds recorded by the 4 am radiosonde launched from Muscat airport.

The observed positive gauge-day rainfall from all the footprints defined over the trial (referred to as the downwind rainfall in what follows) are used to fit a statistical model that controls for expected 'natural' rainfall (i.e. rainfall that would have occurred if there had been no ground-based ionisation) and includes parameters that characterise separate enhancement effects due to operation of the different ionisers over the period of interest. The estimated values for these parameters are used to estimate the total amount of rainfall in the different footprints attributable to the operation of ground-based ionisation over the period of interest following the methodology outlined in Section 2. This estimate is expressed as a percentage of the corresponding estimate of the total natural downwind rainfall over the same period. This is referred to as the ionisation attribution in what follows.

To implement this headline analysis, the 9 119 (out of 122 259) gauge-day measurements corresponding to positive rainfall values over 2013–2018 were classified as

- downwind of the site of a deployed ioniser on the day: that is, in a 30 km wide and 70 km long corridor oriented in the direction of the steering wind on the day, and with the site centred on the starting edge of the corridor. There are 4 168 such gauge-day values;
  - downwind gauge-day values are designated as target values if they are from a gauge downwind of an active site on the day. Note that gauge-day values can be simultaneously downwind of multiple active sites. There are 2 176 such values;
  - the 1 992 remaining downwind gauge-day values that are not target values are designated as control values;
- upwind of the site of a deployed ioniser on the day: that is, in a 30 km wide and 70 km long windward corridor as specified earlier, while not being simultaneously downwind of any other deployed ioniser site. There are 1 545 such gauge-day values; and
- out of scope: neither upwind nor downwind of a deployed ioniser site on the day. There are 3 406 such gauge-day values.

Downwind rainfall was observed for at least one downwind gauge-day on 488 of the 740 days of the trial (no rain was recorded anywhere downwind on the other 252 days). This represents just under 3.5% of the total of 122 259 rainfall measurements recorded 2013–2018. These data are modelled as the outcome of a hurdle process, defined by the joint realisation of a binary variable defined by rainfall occurrence at the gauge on the day, and the positive rainfall reading if in fact there is rainfall. Past Australian trials had shown that rainfall occurrence events are essentially independent of the operating status of an ioniser. Consequently, estimation of the potential rainfall enhancement effect was confined to positive rainfall values, which are mostly made up of natural rainfall, that is, rain that would have occurred in any case. These positive rainfall values were converted to a natural logarithmic scale to reduce the level of skewness in the data and to reduce the influence of very large rainfall measurements, which occur irregularly and are assumed to be independent of the operating status of the ground-based ionisation systems.

These positive rainfall values were modelled in two stages:

1. gauge-day data from the 70 km corridors that were upwind of the deployed ioniser sites each day were used to model the logarithm of the observed natural rainfall at these gauges (i.e. their *LogRain* values) as a linear function of daily meteorological variables and gauge elevation, plus random day and individual gauge-day effects. Table 3 shows the parameter estimates for this model. These were used to calculate an estimate of the expected value of the natural gauge-day value of *LogRain* downwind of the ioniser sites that reflects the

meteorological and orographic processes driving upwind gauge-day natural rainfall. Because only upwind gauge-day rainfall values were used to fit the upwind model, the estimated parameters of this model, and estimates of natural rainfall based on them, are independent of ioniser operation;

2. downwind gauge-day *LogRain* values were modelled as a linear function of their estimated expected values assuming they are natural rainfall values (using the upwind model fitted at stage one), gauge elevation and an indicator variable for each ioniser which, for each gauge-day value, was set to one if the gauge-day value was a target value for that ioniser, that is, it was in the ioniser's footprint and the ioniser was operational that day. Otherwise, the indicator variable took the value zero. By construction, these indicators were all zero for gauge-day values that are controls. In what follows, we refer to these indicators as target status indicators. There is one target status indicator for each ioniser. Table 4 shows the parameter estimates for the downwind model used in this headline analysis.

The *t*-statistics, or |*t*-stat|, values shown in Tables 3 and 4 are significance diagnostics, with |*t*-stat| greater than 2 indicating a highly significant estimate, and |*t*-stat| between 1.8 and 2 indicating a marginally significant estimate. As one would expect, the parameter for *Expected natural rain* in Table 4 is far and away the most significant term in the downwind rainfall model. We can also see that the target indicators for H1, H2, H3 and H5 are highly significant and positive, while the terms for *Gauge elevation* and the interaction term *Elevation*H2 target* are both marginally significant and negative. The negative sign on *Gauge elevation* is not unexpected because it is compensating for the large positive contribution of elevation to *Expected natural rain* (Table 3). In the case of H1, the *Elevation*H1 target* interaction term is small relative to the coefficient for *H1 target indicator* and so has little impact on the overall contribution of a gauge-day reading being a H1 target reading to the downwind rainfall model. This is not the case with H2, where we see that the coefficient for *Elevation*H2 target* is quite close in absolute value to that of *H2 target indicator*, implying that the overall contribution to the downwind rainfall model from a gauge-day reading being a H2 target is quite small. It is also interesting to note that the coefficients for both *H4 target indicator* and *H6 target indicator* are negative, implying that more control rainfall than target rainfall was observed downwind from H4 and H6. The impact of the staggered deployment of H1–H10 is also evident, with smaller numbers of gauge-day readings classified as targets for H7–H10, and consequently less significant results for these sites.

The methodology described in Section 2 is then used to calculate the headline estimate of the 2013–2018 attribution, that is, the change in positive downwind rainfall caused by operation of the ionisers over this period. This is carried out by putting $\mathbf{z}_{it}$ equal to the vector of covariates

Table 3. *Parameter estimates and associated t-values for the linear mixed model fitted to the logarithm of upwind positive rainfall and used in the headline statistical analysis.*

Covariate	*Estimate*	*/t-stat/*
Constant	−1.440	3.610
Gauge elevation (km)	0.434	5.863
Wind speed (m/s)	−0.096	4.728
Total.totals index	0.033	3.920
PC2 for dry temperature	0.145	2.745
PC1 for relative humidity	0.178	7.968
PC1 for air pressure	−0.052	2.604

Upwind data were available on 292 days, with 1 545 upwind gauge-days recording positive rainfall. PC1 and PC2 stands for the first and second principal components respectively of daily values of meteorological measurements from all AWS providing data on the day.

Table 4. *Parameter estimates and associated t-values for the linear mixed model fitted to the logarithm of downwind positive rainfall and used in the headline statistical analysis.*

Covariate	*Estimate*	*/t-stat/*
Constant	0.280	4.360
Gauge elevation (km)	−0.125	1.903
Expected natural rain	0.856	14.734
H1 target indicator	0.289	2.124
H2 target indicator	0.258	2.084
H3 target indicator	0.238	2.576
H4 target indicator	−0.153	1.717
H5 target indicator	0.433	3.282
H6 target indicator	−0.203	1.362
H7 target indicator	0.222	1.184
H8 target indicator	0.059	0.460
H9 target indicator	0.481	1.574
H10 target indicator	0.034	0.206
Elevation*H1 target*	−0.087	−0.603
Elevation*H2 target*	−0.217	−1.812

Expected natural rain is the value of the upwind model fit. Downwind data were available on 488 days, corresponding to 4 168 values of positive rainfall on downwind gauge-days.

*Interactions of elevation with H3 target—H10 target were insignificant and excluded from the model specification.

Table 5. *Summary values of bootstrap distributions generated for headline analysis of 2013–2018 attribution.*

	Average	*Std Dev*	*2.5 percentile*	*97.5 percentile*
Total rainfall (mm)	19 846	2 538	15 715	25 682
Estimated natural rainfall (mm)	17 096	2 296	13 349	22 324
Estimated attributed rainfall (mm)	2 750	565	1 757	3 998
Attribution (%)*	16.23	3.29	10.10	23.09

*As a percentage of estimated natural rainfall and estimated using (5) with $\widehat{\lambda} = 1.092$.

associated with the H1–H10 main effects plus the H1 and H2 elevation interactions in Table 4 and summing values of 5 for all downwind gauge-days reporting positive rainfall over 2013–2018 (Table 5). The uncertainty estimates shown here, including associated significance *P*-values, are computed in two different ways. The first is via bootstrap simulation of downwind positive rainfall, and the second is via random permutation of the 2013–2018 ioniser operating schedule. The bootstrap procedure is aimed at creating an uncertainty distribution for estimated 2013–2018 attribution based on 10 000 independent simulations of the fitted hurdle model for positive downwind rainfall. This is carried out in two steps:

- the first step is a parametric bootstrap simulation of rainfall events over the 43 276 gauge-days that were downwind of the ioniser mechanisms 2013–2018. This is based on fitting a linear-logistic model based on the same covariates as in Table 4 to the binary variable indicating whether rainfall was observed at a downwind gauge-day over 2013–2018. Note that this model is a GLM rather than a GLMM with a random day effect. Ideally one would want to allow for unexplained day to day heterogeneity in rainfall incidence within the bootstrap. However, fitting a GLMM within this bootstrap proved to be unfeasible due to the quite time-consuming fitting process and the fact that the GLMM does not converge when fitted to the actual 2013–2018 data.

- the second step is a two-level semiparametric block bootstrap simulation (Chambers & Chandra, 2013) of *LogRain* for all downwind gauge-days that were simulated in step one as recording rain. This bootstrap is robust to specification of the distribution of residuals within days, including the presence of spatial correlation. Given these simulated *LogRain* values, the downwind model 2 was refitted, and a new headline estimate of the total attributed rainfall was calculated. The distribution of these bootstrap estimates is shown in the left panel of Figure 7.

The main uncertainty measures derived from this bootstrap distribution are the proportion of bootstrapped attribution values that are less than or equal to zero and the interval from the 2.5 bootstrap percentile to the 97.5 bootstrap percentile. We refer to the former as the bootstrap *P*-value for a positive attribution, and the latter as the bootstrap 95% confidence interval (95% CI) for the actual attribution. Summary values of bootstrap distributions are shown in Table 5. Not surprisingly, given that the bootstrap 95% CI for attribution ranges from 10.10 to 23.09, the headline analysis value of attribution has a *P*-value that is less than 0.0001.

A referee has pointed out that temporal and spatial correlations are expected for daily rainfall measurements in a network of gauges. Spatial correlations also exist in our data but are either small for downwind rainfall events or not significant for downwind values of *LogRain*. Furthermore, temporal autocorrelation in the models fitted at both steps is in large part accounted for by the inclusion of the upwind model-based covariate *Expected natural rain* in these models.

A randomised permutation analysis of the impact of the ioniser operating schedule on estimated attribution allows a second *P*-value to be computed for this estimate. This is based on the premise that if ioniser operation does nothing to enhance rainfall, then their operating sequence should have no impact on attribution. It implies that the observed attribution is unlikely to be very different from the attribution obtained if one reanalysed the 2013–2018 data after replacing the actual operating sequence by a different, permuted, version. This is implemented by associating alternative daily operating sequences with each gauge-day. These alternative daily

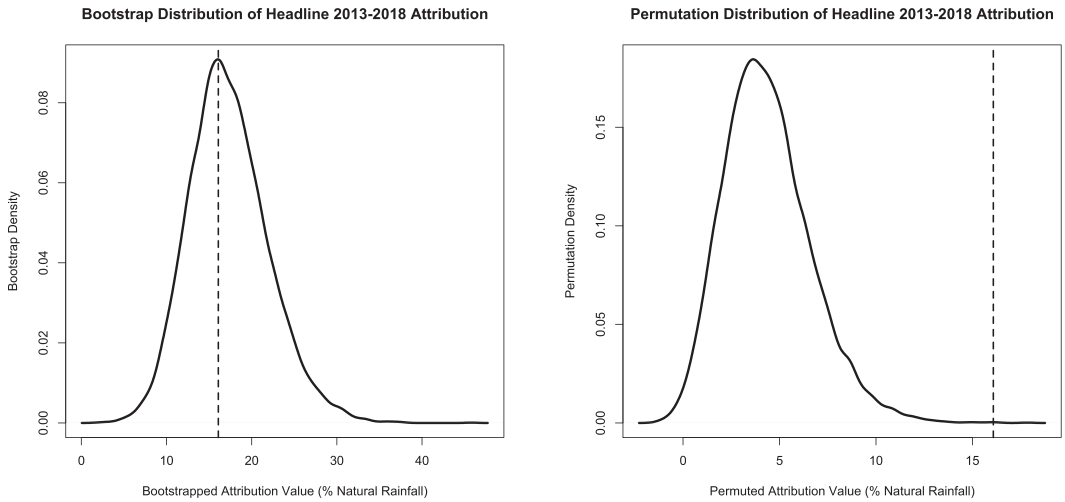

Figure 7. *Bootstrap distribution (left panel) and permutation distribution (right panel) underpinning the uncertainty estimates for the headline analysis of 2013–2018 attribution. The vertical dashed line in both plots is the actual attribution estimate. The bootstrap P-value for attribution (left plot) is <0.0001, and the permutation P-value for attribution (right plot) is 0.0007.*

operating sequences are constructed by first randomly permuting ioniser operating states for each day separately for each gauge-day within a year, then randomly permuting these sequences between gauge-days for each year. This ensures that on any day half of the deployed ionisers for the corresponding year are classified as operating and half as non-operating for each gauge-day. This defines new target and control statuses for downwind gauge-day rainfall, enabling a permuted attribution to be calculated. A large number (10 000) of such permutations are carried out, and the resulting distribution of permuted attribution estimates is compared with the actual attribution estimate. If there is no effect, one would expect the actual attribution estimate to lie somewhere in the 'body' of this permutation distribution. The right panel in Figure 6 shows this permutation distribution, with the actual attribution estimate superimposed. Its permutation *P*-value, that is, the proportion of permuted attribution estimates greater than the one actually observed, is 0.0007. It is extremely unlikely that the attribution estimate we observed could have been obtained by chance. Note that the distribution shown in Figure 6 has a mean value that is positive. This is consistent with the permutations introducing measurement error for the covariates associated with ioniser operation in the model for *LogRain*. This attenuates, but does not zero, the estimated coefficients associated with these covariates, and so reduces, but does not eliminate, the estimated attribution.

5.2 An After the Event Statistical Analysis

The methodology for the headline analysis of the 2013–2018 Hajar Mountains trial was specified before commencement of the trial and is essentially the same as the methodology used to analyse the 2010 trial in South Australia. The main departure from that approach was specification of the footprint, which was changed following inspection of wind speed and direction data collected in 2013, and prior to modelling of the rainfall data collected that year. The other change of any consequence was the inclusion of target-elevation interaction terms in the model used for downwind rainfall. These interactions were highly significant in 2013, and so were retained in the downwind model used to analyse data collected over 2014–2018.

Following the completion of the 2013–2018 trial, it is interesting to revisit the model specification process for *LogRain* using the entire 2013–2018 rainfall data to see if 'better' models for both upwind and downwind rainfall suggest themselves, and to then redo the attribution analysis summarised in Table 5 and Figure 6. To start, we see in Figure 8 that the drying out of the Hajar Mountains region over 2013–2018 that was noted earlier in Figure 6 is evident when we look at positive rainfall summaries on an annual basis, with 2013–2015 much wetter than 2016–2018. Whether this was due to ongoing climate change leading to an increasing drying out of the Persian Gulf and the northern Indian Ocean, or more 'local', and maybe cyclical, medium-term shifts in rainfall patterns over the Hajar Mountains, is unknown. However, it suggests that models for *LogRain* would benefit from inclusion of indicator variables for the different years.

In Figure 9, we show the linear relationship between gauge elevation (in km units) and gauge-day values of *LogRain* over 2013–2018 separately for gauges with elevations at 1 km or less and gauges at greater than 1 km. Although rainfall generally tends to increase with increasing elevation, this changes at around 1 km, with rainfall tending to decrease at higher elevations. However, because the gauges deployed in the second half of the trial were mostly at elevations of less than 500 m, lower elevation gauge deployment later in the trial could have been a factor contributing to the rainfall decline in the last 3 years of the trial (Figure 8). In terms of assessing whether operation of the ioniser mechanisms was an important factor for rainfall enhancement during the trial, it therefore seems reasonable to carry out separate

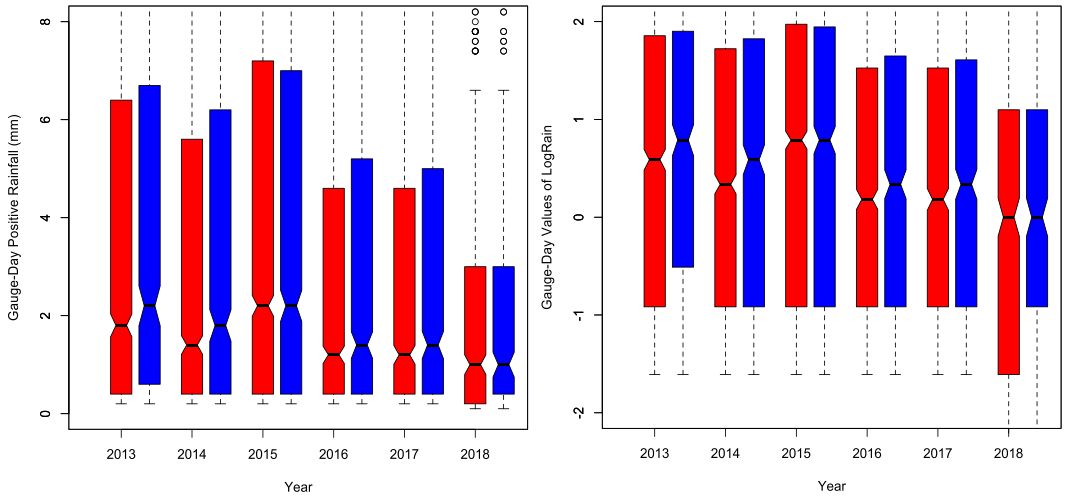

Figure 8. *Interquartile boxes defined by the distribution of gauge-day positive rainfall (mm) by year for the gauge network in the Hajar Mountains. Median values are shown by notches. The plot on the left is for gauge-day positive rainfall, while the plot on the right is for LogRain. Within a plot, the leftmost box for each year is for all gauge-days, while the rightmost box is for downwind gauge-days. The division between 2013–2015 as 'wet' years and '2016–2018' as 'dry' years is apparent. Some care with interpretation is required; however, since over 2013–2018, the gauge network grew from 120 gauges in the central part of the Hajar Mountains region to 201 gauges spread more widely across the region (Figure 3).*

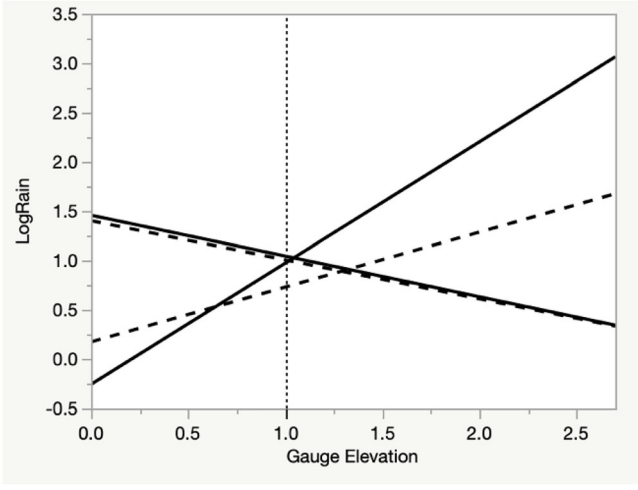

Figure 9. *Plot showing linear least squares fits of gauge-day values of LogRain by gauge elevation. The upward sloping solid line is for all gauge-days with positive rainfall where the gauge is at an elevation of 1 km or less, while the downward sloping solid line corresponds to gauge-days with positive rainfall where the gauge is at an elevation of greater than 1 km. The upward sloping dashed line and the downward sloping dashed line are the same two fits restricted to downwind gauge-days. The vertical dotted line delineates gauges at elevations of 1 km or less from gauges at greater elevations. Over 2013–2018, there were nine gauges at elevations greater than 1 km, and these recorded rainfall on 874 occasions. In contrast, there were 204 gauges at elevations of 1 km or less, and these recorded rainfall on 8 245 occasions.*

analyses for the wetter years 2013–2015 and the drier years 2016–2018, allowing for different effects of high gauge elevation (>1 km) compared with low gauge elevation (<1 km) on gauge level rainfall measurement.

The most important factor in the model fitted to the downwind values of *LogRain* (Table 4) is *Expected natural rain*. This variable is calculated using the fitted model for the upwind values of *LogRain* (Table 3). Intuitively, one would expect the coefficient for this variable in the downwind *LogRain* model to be close to 1. However, from Table 4, we see this is not the case. One possible reason is that the upwind model coefficients are fitted using upwind data that include data from 2013, when the contributing upwind gauge-days are at a much higher elevation compared with upwind gauge-days in subsequent years. In fact, upwind gauge-days in 2013 are at a higher elevation than the downwind gauge-days in 2013, something that is not the case 2014–2018 (Figure 10).

The main impact of 2013 upwind gauge-days being at a much higher elevation than 2014–2018 upwind gauge-days is that the upwind model that includes 2013 data puts a greater emphasis on elevation as a determinant of the gauge-day values of *LogRain*, at the expense of other meteorological variables, particularly *Total totals*. Consequently, it seems appropriate to exercise caution and exclude 2013 gauge-day data from the upwind model fit used to calculate the values of *Expected natural rain* in the downwind model for 2013–2018 values of *LogRain*.

Taken together, these analyses suggest that the models used for both upwind and downwind gauge-day modelling of *LogRain* would benefit from

- inclusion of year effects;
- separation of the effect of increasing elevation on *LogRain* into two terms, one for gauge-days at elevations less than 1 km, and the other for gauge-days at elevations greater than 1 km;
- exclusion of 2013 values from the data used to fit the upwind model for LogRain; and
- separate models fitted to data from 2013–2015 and 2016–2018.

Table 6 shows the estimated parameter values that result when we make the corresponding changes to the specification of our models for downwind values of *LogRain*. To start, we can compare Table 4 with the 2013–2018 columns of Table 6. Here, we see that the main impact of the changes to the specification of the 2013–2018 *LogRain* model is to show that rainfall enhancement from operation of both H1 and H2 is greater for higher altitude gauges, while the coefficient for *Expected natural rain* is substantially closer to one. Table 6 also shows separate

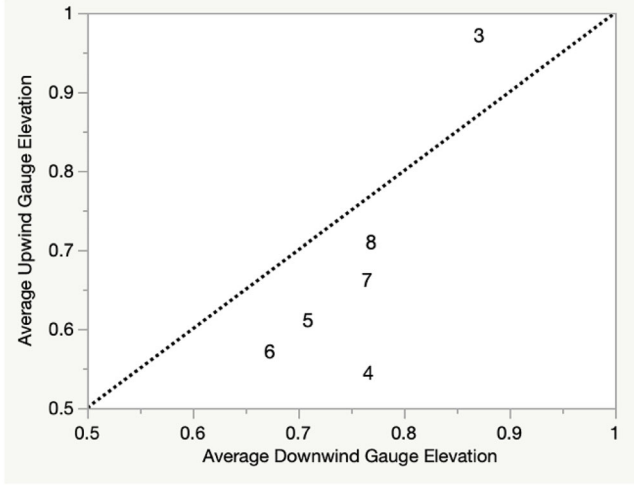

Figure 10. *Average elevations (km) for upwind and downwind gauge-days for each year 2013–2018. Note that the value for each year is denoted by its last integer. Thus, '3' denotes 2013 and so on.*

Table 6. *Parameter estimates and associated t-values for the linear mixed models fitted to downwind LogRain in the after the event statistical analysis.*

Covariate	*2013–2018*		*2013–2015*		*2016–2018**	
	Estimate	*/t-stat/*	*Estimate*	*/t-stat/*	*Estimate*	*/t-stat/*
Constant	0.077	0.633	0.024	0.155	0.345	2.087
Year = 2013	0.406	3.584	0.477	4.018		
Year = 2014	0.336	3.156	0.273	2.501		
Year = 2016	0.259	2.243			0.170	1.436
Year = 2017	0.092	0.774				
Year = 2018	0.041	0.277			−0.057	0.392
Gauge elevation* (<1 km)	−0.200	1.217	−0.061	0.277	−0.472	2.051
Gauge elevation* (>1 km)	−0.096	1.358	−0.085	0.861	−0.071	0.763
Expected natural rain	0.945	15.997	0.883	12.206	1.056	10.689
H1 target indicator	0.481	1.946	0.549	1.817	0.268	2.183
H2 target indicator	0.840	2.868	0.949	2.611	−0.027	0.218
H3 target indicator	0.241	2.614	0.413	3.291	0.054	0.400
H4 target indicator	−0.114	1.284	−0.166	1.374	−0.045	0.344
H5 target indicator	0.499	3.790	0.704	3.052	0.433	2.703
H6 target indicator	−0.136	0.916	−0.349	1.552	0.005	0.023
H7 target indicator	0.336	1.786			0.332	1.758
H8 target indicator	0.132	1.024			0.130	1.005
H9 target indicator	0.711	2.321			0.674	2.195
H10 target indicator	0.196	1.150			0.186	1.087
Elev*(<1 km)*H1 target	−0.488	1.342	−0.599	1.377		
Elev*(<1 km)*H2 target	−1.272	2.715	−1.350	2.312		
Elev*(>1 km)*H1 target	−0.163	1.026	−0.353	1.856		
Elev*(>1 km)*H2 target	−0.458	2.668	−0.576	2.678		
No. of days with rainfall	488		286		202	
No. of gauge-day values	4 168		2 447		1 721	
Attribution estimate**	17.64		18.56		17.18	

Expected natural rain is the value of the upwind model fit, which in all cases is the model in Table 3 fitted to upwind *LogRain* over 2014–2018, replacing gauge elevation with gauge elevation (<1 km) and gauge elevation (>1 km), and with the addition of indicator variables for the years 2014, 2016, 2017 and 2018.

*No interactions between elevation and H1 and H2 target effects fitted because these were essentially zero over 2016–2018.

**As a percentage of natural rainfall.

model fits for 2013–2015 and 2016–2018. Because sample sizes for these fits are smaller, they should be taken as indicative. It is noteworthy that operation of H1, H3 and H5 contribute positively to rainfall enhancement in both periods, while operation of H4 is shown as reducing rainfall in both periods. The reasons for these differences remain unclear at present. However, it is likely that they reflect persistent local orographic features that impact on the operating efficiency of ground-based ionisation at these sites.

The corresponding bootstrap distributions of key downwind rainfall measurements, including the attribution measure, are summarised in Table 7, while in Figure 11, we contrast the bootstrap and permutation distributions of attribution for 2013–2015 and 2016–2018. The calculated attribution is significantly greater than zero (in fact, it is significantly greater than 10%), with permutation *P*-values of 5% or less, over both periods. That is, the after the event analysis slightly increased our estimate of attribution during the Hajar Mountains trial, indicating that it was between 17% and 18% in both the wet (2013–2015) and the dry (2016–2018) periods of the trial.

More detailed after the event analyses of the 2013–2018 data collected in the Hajar Mountains trial are possible, for example, individual year, or individual ioniser, analyses. But the rainfall data for these are sparse, and the statistical reliability of the conclusions that one can draw from them becomes rather weak. Therefore, we do not dwell on them here.

Table 7. *Summary values of bootstrap distributions generated by the after the event analysis of the Hajar Mountains trial data.*

	Average	*Std Dev*	*2.5 percentile*	*97.5 percentile*
2013–2018				
Total rainfall (mm)	19 846	2 158	16 224	24 633
Natural rainfall (mm)	16 870	1 909	13 661	21 145
Attributed rainfall (mm)	2 976	561	2 026	4 188
Attribution (%)*	17.74	3.24	11.79	24.54
2013–2015				
Total rainfall (mm)	12 615	1 570	10 014	16 091
Natural rainfall (mm)	10 640	1 360	8 398	13 658
Attributed rainfall (mm)	1 974	475	1 159	3 023
Attribution (%)*	18.68	4.36	10.83	27.92
2016–2018				
Total rainfall (mm)	7 232	1 375	5 278	10 415
Natural rainfall (mm)	6 171	1 186	4 512	8 857
Attributed rainfall (mm)	1 060	332	547	1 823
Attribution (%)*	17.30	4.65	9.11	27.48

*As a percentage of natural rainfall.

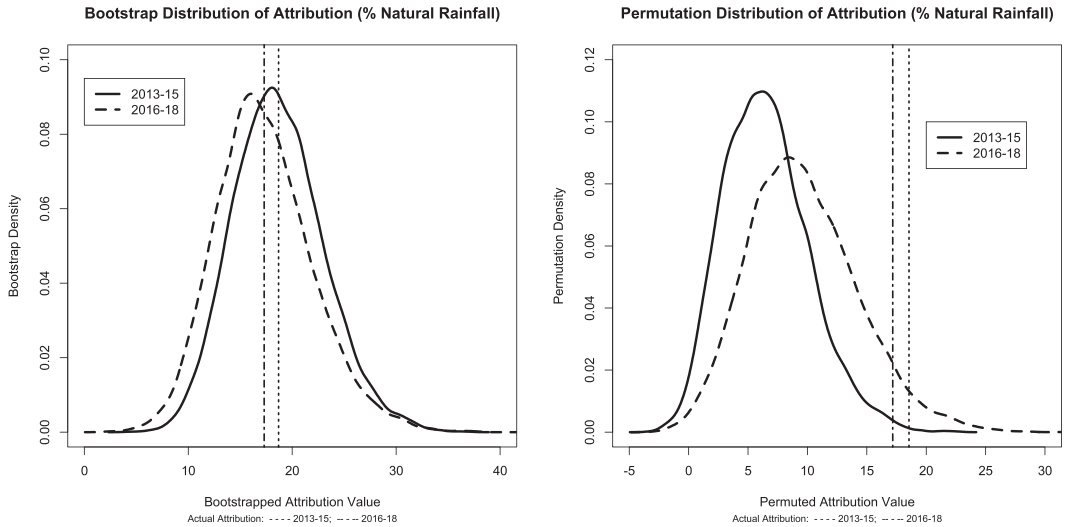

Figure 11. *Bootstrap distributions (left panel) and permutation distributions (right panel) underpinning the uncertainty estimates for the after the event analysis of 2013–2015 and 2016–2018 attributions. The vertical lines in both plots are the actual attribution estimates. The bootstrap P-values for attribution (left plot) are <0.0001 for both 2013–2015 and 2016–2018, and the corresponding permutation P-values for attribution (right plot) are 0.0017 and 0.0589.*

The one extra analysis that is worth commenting on reflects the fact that the data collected in 2013 was 'special', in the sense that meteorological data collected in the 2013 trial dictated the specification of the footprint model used in 2013 and in subsequent years. As we noted earlier, information on daily wind speeds and directions from the radiosonde at Muscat airport collected in 2013 was used to decide on this footprint specification. Even though this decision was made *before* the analysis of any rainfall data from 2013, it could be argued that the data collected in 2013 should not be included in a formal analysis of the impact of ground-based ionisation on rainfall in the Hajar Mountains. This also accords with the decision to not use the 2013 upwind rainfall data in the after the event analysis. We do not provide the full details for both the

headline and the after the event analyses of the 2014–2018 data here, merely noting that exclusion of the 2013 data stabilises both sets of results, leading to a headline attribution estimate of 18.76% (bootstrap *P*-value and permutation *P*-value both less than 0.0001) and an attribution estimate of 20.92% (bootstrap *P*-value and permutation *P*-value both less than 0.0001) from an after the event analysis.

6 Is Rainfall Enhancement Via Ground-Based Ionisation Still a Pseudo-Science?

The results from the statistical analysis of the 2013–2018 Hajar Mountains trial described in the previous section seem clear cut. In particular, there appears to be considerable statistical evidence that ionisation of aerosols carried aloft in the strong updrafts characteristic of the slopes of the Hajar Mountains in summer leads to increased rainfall from the moisture-laden convective clouds that form over these slopes at that time. The precise amount of rainfall enhancement is obviously subject to some uncertainty, and varies from location to location, but an enhancement of at least 10–15% is highly likely given the conditions that were prevalent over 2013–2018. This has quite significant implications for increasing water security in what is an extremely arid part of the world.

However, this claim still needs to be recognised as valid by the scientific community. In this context, it is interesting to see how it stacks up against the requirements for a 'proper' scientific evaluation of a rainfall enhancement trial that were laid out in the World Meteorological Organisation's 2010 review of rainfall enhancement (WMO, 2010). These are (our italics)

1. a *randomization* process in the experimental design such that only some of the events suitable for seeding are in fact seeded. This requires objective criteria defining the start of an event so that bias is not introduced by subjective selection of seeded and unseeded events;
2. a primary analysis (where) the impact of seeding is assessed through various *objective statistical techniques* that compare unseeded events to seeded events and provide an *estimate of the precipitation increase* along with the *confidence intervals* in which the true impact lies;
3. *physically-based secondary analyses* aimed at ensuring that the seeding hypothesis is validated. (These) secondary analyses provide physical support for the primary analysis, by explaining the *scientific basis* of the statistical result; and
4. due to the large natural variability (of rainfall) it is important to emphasise that weather modification programmes should be viewed a *long-term (multi-year) commitment* to be able to scientifically evaluate these experiments.

It is obvious that the 2013–2018 Hajar Mountains trial of rainfall enhancement via ground-based ionisation has met requirements 1, 2 and 4. The one requirement that has not been met is 3. This requirement implies that as far as the WMO is concerned (and, one assumes, scientists who adhere to the WMO's viewpoint), application of valid (and replicable) statistical design and analysis methods to empirically verify a claimed rain enhancement effect is never enough. The causal mechanism for the enhancement process should itself be empirically verified. But direct measurement of the role of ionised aerosols in encouraging raindrop coalescence in the natural conditions that occur in the Hajar Mountains is impossible (or at least economically unfeasible) given current technology. Consequently, the use of ground-based ionisation as a rainfall enhancement method remains in scientific limbo—we know it works in appropriate situations, but we cannot show physical evidence of it working (i.e. we cannot show ionisation of cloud droplets and their resulting coalescence into raindrops). From this viewpoint, one therefore must answer 'yes' to the question posed in the title of this section.

But science never stands still and our capacity to address requirement 3 may soon change (Zheng *et al*., 2020, and Zhang *et al*., 2020). It is also worth noting that much of what is recognised as 'real science' still fails requirement 3 (Johnson, 2015).

Irrespective of these issues, the data obtained in the Hajar Mountains trial and the subsequent statistical analysis has considerably improved our knowledge of the impact of ground-based ionisation on rainfall enhancement. We know that for situations like those in the Hajar Mountains, investigation of whether rainfall enhancement works or not requires large data sets and complex analysis. But this means deep pockets (and long planning horizons) are necessary to obtain the required data. Here, the 2013–2018 Hajar Mountains trial provides an example of what is possible in this regard. We also know that correlation, however strong it appears in our analysis, is not causation. But it is an extremely good indicator that something is going on. We also know that replication is an even better indicator. In this context, it is heartening that the Oman Government has now incorporated ground-based ionisation technology into its water infrastructure planning and is carrying out further experimentation. Finally, we should note that the trial reports are freely available (https://www.australianrain.com.au/resources), with the data used in the analyses reported in this paper included in the supporting information. Availability of these data should be a strong incentive for further research. But it is very difficult, even with good statistical results, to change entrenched scientific opinion, and much more work remains to be carried out. Unfortunately, this becomes difficult when unsupported pseudo-scientific claims about the use of ionisation for rainfall enhancement are made by commercial interests. But there is ongoing work aimed at improving our understanding of the use of ground-based ionisation for rainfall enhancement in other parts of the world (Zheng *et al*., 2020), as well as improving our ability to use ionisation more generally as a rainfall enhancement strategy (Zhang *et al*., 2020). It seems that although ionisation-based rainfall enhancement is still a pseudo-science, it is one that statistics is helping 'nudge' towards a science.

References

Chambers, R., Beare, S. & Peak, S. (2012). Using dynamically defined controls to evaluate the impact of an ionization technology. *J. Weather Modif.*, **44**, 16–29.

Chambers, R. & Chandra, H. (2013). A random effect block bootstrap for clustered data. *J. Comp. Graph. Statist.*, **22**, 452–470.

Charabi, Y. (2013). Projection of future changes in rainfall and temperature patterns in Oman. *J. Earth Sci. Clim. Change*, **4**, 154.

Dempewolff, R.F. (1959). High voltage rainmakers. *Popular Mechanics*, **111(3), 81-85**, 252–255.

Doshi, N. & Agashe, S. (2015). Feasibility study of artificial rainfall system using ion seeding with a high voltage source. *J. Electrostat.*, **74**, 115–127. https://doi.org/10.1016/j.elstat.2015.01.005

Duan, N. (1983) Smearing estimate: A nonparametric retransformation method. *Journal of the American Statistical Association*, **78**, 605–610.

Fajardo, C., Costa, G., Ortiz, L.T., Nande, M., Rodríguez-Membibre, M.L., Martín, M. & Sánchez-Fortún, S. (2016). Potential risk of acute toxicity induced by AgI cloud seeding on soil and freshwater biota. *Ecotoxicol. Environ. Safety*, **133**, 433–441. https://doi.org/10.1016/j.ecoenv.2016.06.028

Fletcher, N.H. (2013). Effect of electric charge on collisions between cloud droplets. *J. Appl. Meteor. Climatol.*, **52**, 517–520. https://doi.org/10.1175/JAMC-D-12-093.1

Fletcher, N.H. (2014). Reply to "Comments on 'Effect of Electric Charge on Collisions between Cloud Droplets"'. *J. Appl. Meteor. Climatol.*, **53**, 1321.

Flossmann, A.I., Manton, M., Abshaev, A., Bruintjes, R., Murakami, M., Prabhakaran, T. & Yao, Z. (2018). *Peer Review Report on Global Precipitation Enhancement Activities*. World Meteorological Association, WWRP 2018–1, Geneva.

French, J.R., Friedrich, K., Tessendorf, S.A., Rauber, R.M., Geerts, B., Rasmussen, R.M., Xue, L., Kunkel, M.L. & Blestrud, D.R. (2018). Precipitation formation from cloud seeding. *PNAS*, **115**(6), 1168–1173. https://doi.org/10.1073/pnas.1716995115

Hannaford, S. (2015). Concerns persist over long-term impact of cloud seeding in Kosciuszko. https://www.smh.com.au/technology/concerns-persist-over-longterm-impact-of-cloud-seeding-in-kosciuszko-20150303-13tj6c.html

Hsu, J. & Bryner, J. (2011). Rainmaking in Middle Eastern Desert: success or scam? https://www.livescience.com/10398-rainmaking-middle-eastern-desert-success-scam.html

Johnson, C.Y. (2015). One big myth about medicine: we know how drugs work. https://www.washingtonpost.com/news/wonk/wp/2015/07/23/one-big-myth-about-medicine-we-know-how-drugs-work/

Levin, Z. (2009). On the state of cloud seeding for rainfall enhancement. *Climate Change and Impacts in the Eastern Mediterranean and Middle East Project, Energy, Environment and Water Research Center (EEWRC)*. Cyprus Institute.

List, R. (2005). The serious flaws of the Academies' report on weather modification research. *J. Weather Modific.*, **37**, 67–70.

Manton, M.J., Peace, A.D., Kemsley, K., Kenyon, S., Speirs, J.C., Warren, L. & Denholm, J. (2017). Further analysis of a snowfall enhancement project in the Snowy Mountains of Australia. *Atmos. Res.*, **193**, 192–203. https://doi.org/10.1016/j.atmosres.2017.04.011

NRC (2003). *Critical Issues in Weather Modification Research*. National Academy Press, Washington, DC.

Rasmussen, R.M., Tessendorf, S.A., Xue, L., Weeks, C., Ikeda, K., Landolt, S., Breed, D., Deshler, T. & Lawrence, B. (2018) Evaluation of the Wyoming Weather Modification Pilot Project (WWMPP) using two approaches: traditional statistics and ensemble modeling. *J. Appl. Meteor. Climatol.*, **57**, 2639–2660.

Tinsley, B.A. & Zhou, L. (2014). Comments on "Effect of Electric Charge on Collisions between Cloud Droplets". *J. Appl. Meteor. Climatol.*, **53**, 1317–1320.

US Marine Corps (1990). *The Persian Gulf Region, A Climatological Study. Department of the Navy United States Marine Corps Operational Handbook 0–54, Fleet Marine Force Reference Publication*: Washington, DC.

Vonnegut, B., Maynard, K., Sykes, W.G. & Moore, C.B. (1961). Technique for introducing low-density space charge into the atmosphere. *J. Geophys. Res.*, **66**, 823–830.

Vonnegut, B. & Moore, C.B. (1959). Preliminary attempts to influence convective electrification in cumulus clouds by introduction of space charge into the lower atmosphere. In *Recent Advances in Atmospheric Electricity*, Pergamon Press, London, 317–322.

Vonnegut, B., Moore, C.B., Semonin, R.G., Bullock, J.W., Staggs, D.W. & Bradley, W.E. (1962b). Effect of atmospheric space charge on initial electrification of cumulus clouds. *J. Geophys. Res.*, **67**, 3909–3922.

Vonnegut, B., Moore, C.B., Stout, O.E., Staggs, D.W., Bullock, J.W. & Bradley, W.E. (1962a). Artificial modification of atmospheric space charge. *J. Geophys Res.*, **67**, 1073–1083.

Wang, P., Li, C., Li, J., Zhang, M., Yang, Y. & Yu, K. (2020b). Electrostatic effects of corona discharge on the spectrum and density evolution of water droplets in air. *IEEE Access*, **8**, 196264–196273. https://doi.org/10.1109/ACCESS.2020.3034264

Wang, P., Li, C., Zhang, M., Yang, Y. & Yu, K. (2020a). Density enhancement of nano-sized and submicron-sized water droplets induced by charges released from corona discharge. *J. Physics D: Appl. Physics*, **53**, 445203.

WMO (2007). WMO Statement on Weather Modification. The commission for atmospheric sciences management group, second session, Oslo, Norway, 24–26 September 2007. CAS-MG2/Doc 4.4.1, Appendix C.

WMO (2010). WMO Statement on Weather Modification. Expert Team on Weather Modification Research, Abu Dhabi, 22–24 March.

Yang, Y., Tan, X., Liu, D., Lu, X., Zhao, C., Li, J. & Pan, Y. (2018). Corona discharge-induced rain and snow formation in air. *IEEE Trans. Plasma Sci.*, **46**, 1786–1792.

Zhang, M., Han, F., Wang, P., Qian, C., Li, C., Yang, Y. & Yu, K. (2020). Numerical analysis of charged particles transport in air based on vortex rings. *IEEE Access*, **8**, 160891–160896. https://doi.org/10.1109/ACCESS.2020.3020722

Zheng, W., Xue, F., Zhang, M., Wu, Q., Yang, Z., Ma, S., Liang, H., Wang, C., Wang, Y., Ai, X., Yang, Y. & Yu, K. (2020). Charged particle (negative ion)-based cloud seeding and rain enhancement trial design and implementation. *Water*, **12**, 1644. https://doi.org/10.3390/w12061644.

[*Received February 2021; accepted December 2021*]